Muted calcareous nannoplankton response at the Middle/Late Eocene Turnover event in the western North Atlantic Ocean

Cherry Newsam[1], Paul R. Bown[1], Bridget S. Wade[1], Heather L. Jones[2]

With 4 figures and 1 plate

Abstract. Key extinctions in two major planktonic foraminiferal groups and high taxic turnover in radiolarians have led to the identification of the Middle/Late Eocene Turnover (MLET) and point towards significant palaeoclimatic and/or palaeoceanographic changes at around 38 million years ago. Here we present quantitative calcareous nannofossil data from Ocean Drilling Program Site 1052 (Blake Nose, western North Atlantic) in order to investigate the response of phytoplankton during the MLET. Our data show only minor shifts in taxon abundance, with no strong trends identified through the interval and no nannofossil origination or extinction events associated with the MLET. The assemblages are characterised by the dominance of neritic braarudosphaerids and eurytopic reticulofenestrids. The increased abundance of warm to temperate and mesotrophic nannofossils (*Reticulofenestra reticulata, Reticulofenestra bisecta* and *Coccolithus pelagicus*) in and around the MLET occur against a backdrop of cooling, as indicated by oxygen isotopes, suggesting that changing nutrient conditions was the principle driver of these shifts in the nannoplankton assemblage. This is further supported by an increase in radiolarian accumulation rates at this time. The lack of response in the calcareous nannoplankton relative to the zooplanktonic planktonic foraminifera and radiolaria demonstrates the contrasting sensitivity to environmental change in these different plankton groups, with radiolarians showing the highest degree of change at the MLET and the nannoplankton showing little or none.

Key words. Calcareous nannofossils, MLET, palaeoecology, Blake Nose, Ocean Drilling Program, extinction

1. Introduction

The Eocene saw the transition from greenhouse to icehouse climate mode, alongside accompanying palaeoceanographic and biotic change. Peak Paleogene warmth occurred during the Early Eocene Climatic Optimum (52 million years ago (Ma)) followed by cooling through the middle to later part of the Eocene and initiation of Antarctic ice sheet growth by the earliest Oligocene (Zachos et al. 2001). Stable isotope records from the Eocene show high variability over short periods from low, mid and high latitude sites (Okafor et al. 2009) indicating increasing climatic instability, and a number of significant step-like events are superimposed on the broader Eocene cooling trend (Villa et al. 2008). This palaeoclimatic and palaeoceanographic change was accompanied by significant extinctions and turnover in zooplankton groups, with a concentration of extinctions

Authors' addresses:
[1] Department of Earth Sciences, University College London, Gower Street, London, UK, WC1E 6BT
[2] Department of Geosciences, The Pennsylvania State University, University Park, Pennsylvania 16802, USA
E-mail addresses: cherry.newsam.11@ucl.ac.uk; p.bown@ucl.ac.uk; b.wade@ucl.ac.uk; hlj123@psu.edu
Corresponding author: Cherry Newsam, cherry.newsam.11@ucl.ac.uk

around ~ 38 Ma identified as the Middle/Late Eocene Turnover (MLET) event (Kamikuri and Wade 2012). Two major planktonic foraminiferal groups, *Morozovelloides* (formerly *Morozovella*) and large *Acarinina*, disappeared within 10 thousand years (kyr) (Wade 2004, Wade et al. 2012), and a substantial turnover in radiolarians saw the extinction of 13 species and origination of 4 species, in less than 100 kyr (Kamikuri and Wade 2012). The causal factor(s) responsible for the turnover in radiolarians and planktonic foraminifera at ~ 38 Ma is currently uncertain, but at Blake Nose appears to have coincided with an interval of cooling and increased surface water productivity. This may in turn have resulted in biogeographic shifts in radiolarians (Kamikuri and Wade 2012) and triggered symbiont bleaching and dwarfing in planktonic foraminifera (Wade et al. 2008, Wade and Olsson 2009). This interval is also close to the level proposed for the Global Stratigraphic Section and Point (GSSP) for the base of the Priabonian Stage (upper Eocene) (Agnini et al. 2011, Wade et al. 2012).

In this study, we document the calcareous nannofossil record from the MLET at Ocean Drilling Program (ODP) Site 1052, Blake Nose (western North Atlantic Ocean), in order to test for the response of phytoplankton during this interval of significant zooplanktonic turnover. In the Paleogene there is a broad link between nannoplankton diversity (species richness) and climatic trends, and in particular as climate cooled there was significant loss of diversity from a middle Eocene maximum through to a minimum in the Oligocene (Bown et al. 2004, 2008). The middle to late Eocene was therefore one of the most significant intervals of evolutionary turnover for the calcareous nannoplankton, but, as yet, the detail of the rate and structure of this diversity loss is uncertain and the role of the MLET has been untested.

2.   Materials and Methods

2.1   Geological setting

Study samples come from ODP Site 1052, the shallowest site of a depth transect on Blake Nose (western North Atlantic), at a current water depth of 1345 m and
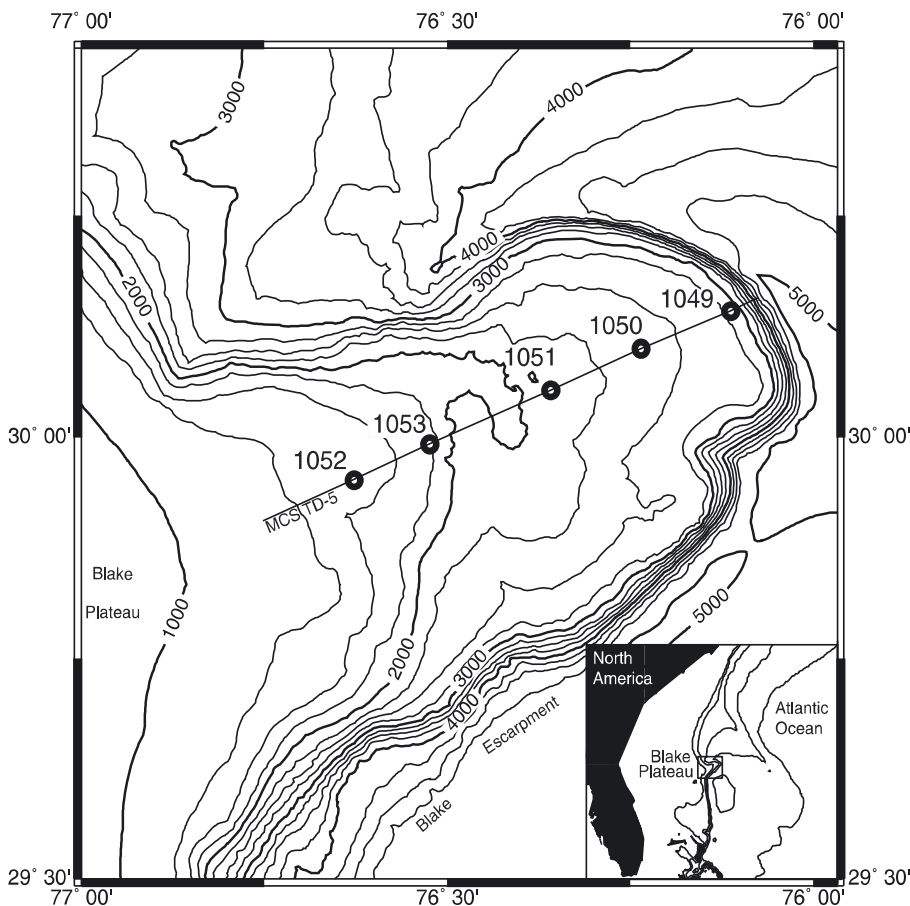

Fig. 1. Location map showing drill locations and bathymetry (m) of Ocean Drilling Program Leg 171B, Sites 1049–1053 on the Blake Plateau (Kroon et al. 1998).

located at 29°57 N, 76°37 W (Fig. 1). Eocene water depth is estimated to have been between 600–1000 m with a palaeolatitude of 29 °N (Norris et al. 1998, Ogg and Bardot 2001). Site 1052 provides a complete middle to upper Eocene section of nannofossil to siliceous nannofossil ooze with relatively well preserved calcareous and siliceous microfossils with magnetostratigraphic and cyclostratigraphic age control (Norris et al. 1998, Ogg and Bardot 2001, Pälike et al. 2001). We have studied the same samples as those used to first document the extinctions in *Morozovelloides* and large *Acarinina* by Wade (2004), from a composite section of holes 1052B and 1052F (85.18 to 111.46 metres composite depth [mcd]), corresponding to 37.58 to 38.35 Ma using the Pälike et al. (2001) timescale.

2.2 Preparation and count techniques

Forty simple smear slides were produced using the technique of Bown and Young (1998). Low-resolution sample spacing ($\sim$ every metre, representing ~ 28 kyr) provides an overview of the background assemblage composition during this interval, and higher resolution analyses (every 10 cm, representing ~ 3 kyr) from 37.82 to 37.79 Ma focus on the MLET itself. Relative abundance counts were performed using a Zeiss Axiophot light microscope (LM) at a magnification of 1000x, using cross polarized, (XPL), bright field (BF) and phase contrast (PC) light microscopy. A minimum of 300 specimens were counted per slide across a random traverse.

Selected samples were also observed using a JEOL JSM-6480LV scanning electron microscope (SEM) including both circular strew slides (Bown and Young 1998) and freshly broken sediment surfaces (Lees et al. 2004). High resolution imaging on the SEM provides a robust assessment of nannofossil preservational state.

2.3 Calcareous nannofossil palaeoecological groups

Variations in nannofossil assemblage composition and diversity can be related to surface water (mixed layer) environmental change, predominantly temperature and nutrients, by analogy with modern ecological observations (Winter et al. 1994). Despite the eurytopic nature of this phytoplankton group some taxa are strongly associated with two end-member palaeoenvironmental groups, the K mode specialists (~oligotrophs) and r mode opportunists (~eutrophs), although many species are considered to be mesotrophs, having relatively broad ecological tolerances (Bralower 2002, Gibbs et al. 2006, Suppl. Info. Table S4). The dominant control on the palaeoecology of extinct taxa is often difficult to determine, as species abundance may reflect the influence of one or more factors (Villa et al. 2008). The interpretation of nannofossil palaeoecology is predominantly based on studies of biogeographical distribution and abundance (Haq and Lohmann 1976, Haq 1980, Roth and Krumbach 1986, Wei and Wise 1990, Wei and Wise 1992) or comparisons with biotic and/or geochemical proxies, of palaeotemperature and palaeoproductivity in particular (Bralower 2002, Villa et al. 2008). Compilations of these interpretations have attempted to extract consensus on species preferences from multiple studies but this is not always straightforward. Although some species are relatively well understood, others appear to have more complex ecologies and previous work has highlighted contrasting opinions (Villa et al. 2008, Bown and Pearson 2009, Schneider et al. 2013).

Grouping the abundance data of species with similar ecological preference has been widely used to provide a broad description of changes in palaeoenvironment (e. g., Wei and Wise 1990, Herrle 2002, Shamrock and Watkins 2012). Here, we use a similar approach with palaeoecological groupings considered to have warm and cool temperature affinities, which also broadly equate to oligotrophic and meso/eutrophic preferences. We have grouped the taxa using previous palaeoecological interpretations with the warm water oligotroph group comprising *Discoaster, Sphenolithus, Umbilicosphaera protoannula* and *Coccolithus formosus* and the cold water eutrophic group comprising *Reticulofenestra lockeri, Reticulofenestra daviesii, Reticulofenestra umbilicus, Chiasmolithus* and *Clausicoccus* (Wei and Wise 1990, Villa et al. 2008). The groups integrate the records of environmentally diagnostic nannoplankton to provide a summary of assemblage changes through the MLET that can be compared with other proxies of environmental change.

2.4 Statistical analysis

In order to test for environmental gradients within the dataset, detrended correspondence analysis (DCA) was performed using R (R Development Core Team 2008). Prior to analysis, the raw nannofossil count data were converted to percentage abundance to account for small differences in sample size. In order to observe which environmental parameters best explain variations between samples along the primary axis (DCA

1), samples were divided into three time bins: pre-MLET (38.4 to 37.9 Ma), MLET (37.9 to 37.76 Ma) and post-MLET (37.76 to 37.5 Ma). DCA sample scores were then coded according to these time bins to determine whether there were significant variations in nannofossil assemblage composition through time. To summarize the impact of environmental variables on the assemblage data, carbon and oxygen isotope vectors were overlain on the DCA ordination using the environmental fit ('envfit') function in the vegan package on R. The length and direction of the vectors produced show the strength of the correlation between a given environmental variable and a DCA axis. DCA 1 sample scores were also plotted against age to assess the variation through time.

3.   Results

3.1   Calcareous nannofossil abundance, preservation and diversity

Calcareous nannofossils are abundant in all samples, with preservation moderate to good throughout, and diversity relatively high (60 species identified across the interval). The samples are dominated by reticulofenestrids with *Reticulofenestra* and *Cyclicargolithus* comprising ~ 40 and ~ 13 % of the assemblages, respectively. Braarudosphaerids and *Coccolithus pelagicus* are also significant components, with averages of ~ 15 and 8 %, respectively. *Discoaster*, *Sphenolithus* and *Zygrhablithus bijugatus* are low in abundance (on average < 5 %) and *Clausicoccus*, *Chiasmolithus*, *Markalius inversus* and *Neococcolithes dubius* are very rare throughout (on average < 1 %). The last occurrence (LO) of *Sphenolithus obtusus* (38.35 Ma) and the acme base (AB) of *Reticulofenestra erbae* (37.58 Ma) place the interval within zones NP17-NP18 of Martini (1971) (Fig. 2) (see also Fornaciari et al. 2010, Agnini et al. 2014).

A visual assessment of the calcareous nannofossil preservation under the LM showed the calcareous nannofossils to be moderately to well preserved throughout the section (Plate 1). This was based on the presence of fine details such as central area grills, which were commonly intact. However the Braarudosphaeraceae species, made up of pentagonal liths, were often fragmented, although this is a common feature of this group. High resolution observation using the SEM showed relatively pervasive overgrowth of the calcareous nannofossils.

The species richness calculated from assemblage abundance counts is relatively consistent throughout (average 33 species), but ranges from 29 to 41 species (Fig. 3), and can vary by 10 species from sample to sample. These large fluctuations most likely reflect the presence of rare taxa. SHE analysis uses the parameters S (number of species), H (information function) and E (measure of evenness), related in the equation $H = \ln S + \ln E$. As the function H uses both number of species and their relative abundances, it allows for evenness and species richness to be examined separately (Buzas and Hayek 1998). The Shannon H and ln (S) values show no significant changes across the interval with Shannon H values between 2.24 and 2.67 and ln (S) between 3.37 and 3.71 (Fig. 3). The two indices show relatively parallel trends, indicating a similar evenness is maintained throughout the interval. Evenness is 0.37 on average, indicating that the assemblage has many species of similar abundances.

3.2   Abundance patterns

Reticulofenestra minuta, the *Reticulofenestra dictyoda* group (*Reticulofenestra dictyoda* 3–14 μm and *Reticulofenestra umbilicus*) and *Cyclicargolithus floridanus* comprise the dominant components of the assemblages at Blake Nose (Fig. 2). *R. minuta* has a high abundance lower in the section but rapidly declines at

Plate 1. LM images (XPL unless otherwise noted) of selected calcareous nannofossil taxa from Blake Nose ODP site 1052. 1. *Pemma basquensis* 1052B–11H-4, 73–76 cm; 2. *Pemma papillatum* 1052B-11H-4, 53–56 cm, a. (XPL) b. (PC); 3. *Micrantholithus* sp. 1052B-11H-4, 133–136 cm; 4. *Micrantholithus* sp. 1052B-11H-4, 73–76 cm; 5. *Micrantholithus* pentaliths 1052B-11H-4, 143–146 cm; 6. Stacked braarudosphaerid 1052B-11H-4, 113–116 cm; 7. *Cyclicargolithus floridanus* 1052F-10H-4, 83–86 cm; 8. *Reticulofenestra bisecta* 1052F-12H-6, 103–106 cm; 9. *Coccolithus pelagicus* 1052F-11H-2, 33–36 cm; 10. *Reticulofenestra reticulata* 1052F-12H-6, 103–106 cm; 11. *Reticulofenestra minuta* 1052B-11H-4, 123–126 cm; 12. *Reticulofenestra lockeri* 1052B-11H-4, 113–116 cm; 13. *Chiasmolithus titus* 1052B-11H-4, 123–126 cm; 14. *Clausicoccus subdistichus* 1052F-10H-3, 103–106 cm; 15. *Coccolithus formosus* 1052B-11H-4, 143–146 cm; 16. *Umbilicosphaera protoannula* 1052F-11H-6, 83–86 cm; 17. *Discoaster barbadiensis* 1052B-11H-4, 73–76 cm, a. (XPL) b. (PC); 18. *Sphenolithus moriformis* 1052B-12H-4, 3–6 cm; 19. *Sphenolithus radians* 1052F-11H-6, 83–86 cm; 20. *Sphenolithus obtusus* 1052F-12H-6, 103–106 cm; 20. *Reticulofenestra erbae* 1052B-10H-2, 63–66 cm.
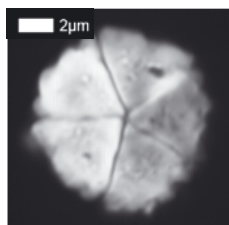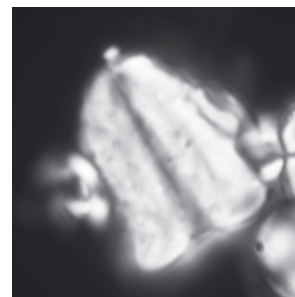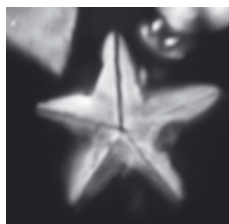
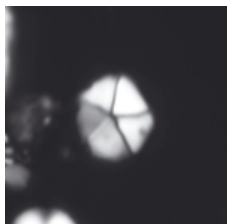*1. Pemma basquensis*
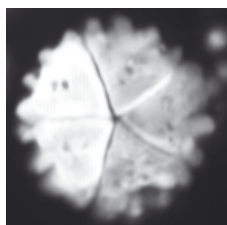
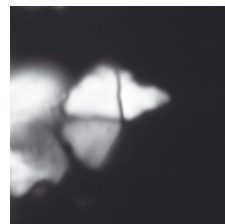*2a. Pemma papillatum*

2b. Pemma papillatum
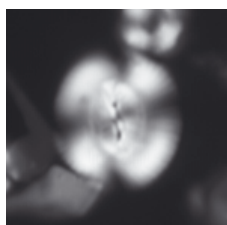
6. Stacked braarudosphaerid
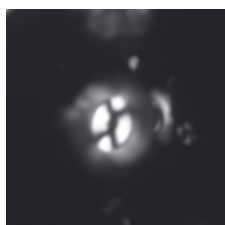
3. Micrantholithus sp.

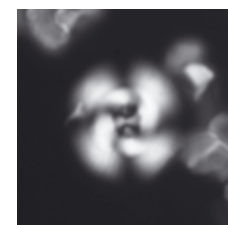*4. Micrantholithus* sp.

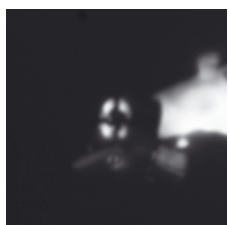*5. Micrantholithus* pentaliths

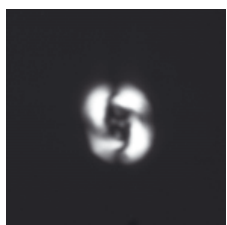*7. Cyclicargolithus
floridanus*

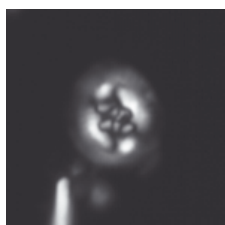*8. Reticulofenestra
bisecta*

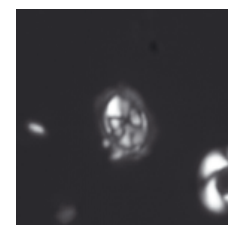*9. Coccolithus pelagicus*

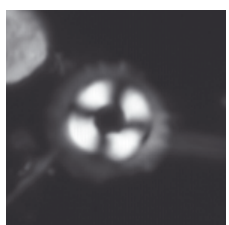*10. Reticulofenestra
reticulata*

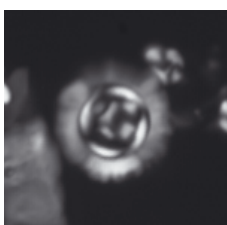*11. Reticulofenestra
minuta*

*12. Reticulofenestra
lockeri*

*13. Chiasmolithus
titus*

*14. Clausicoccus
subdistichus*

*15. Coccolithus
formosus*

*16. Umbilicosphaera
protoannula*
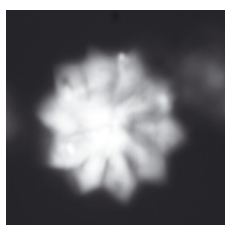
17a. Discoaster barbadiensis
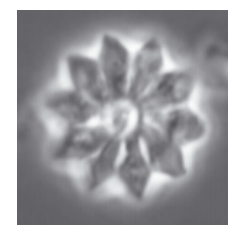
17b. Discoaster barbadiensis

*18. Sphenolithus
moriformis*
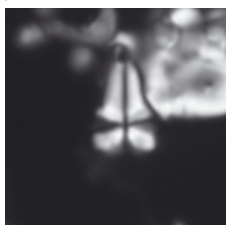
*19. Sphenolithus
radians*
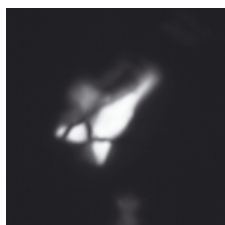
*20. Sphenolithus
obtusus*
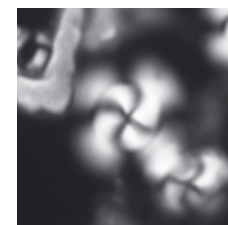
*21. Reticulofenestra
erbae*
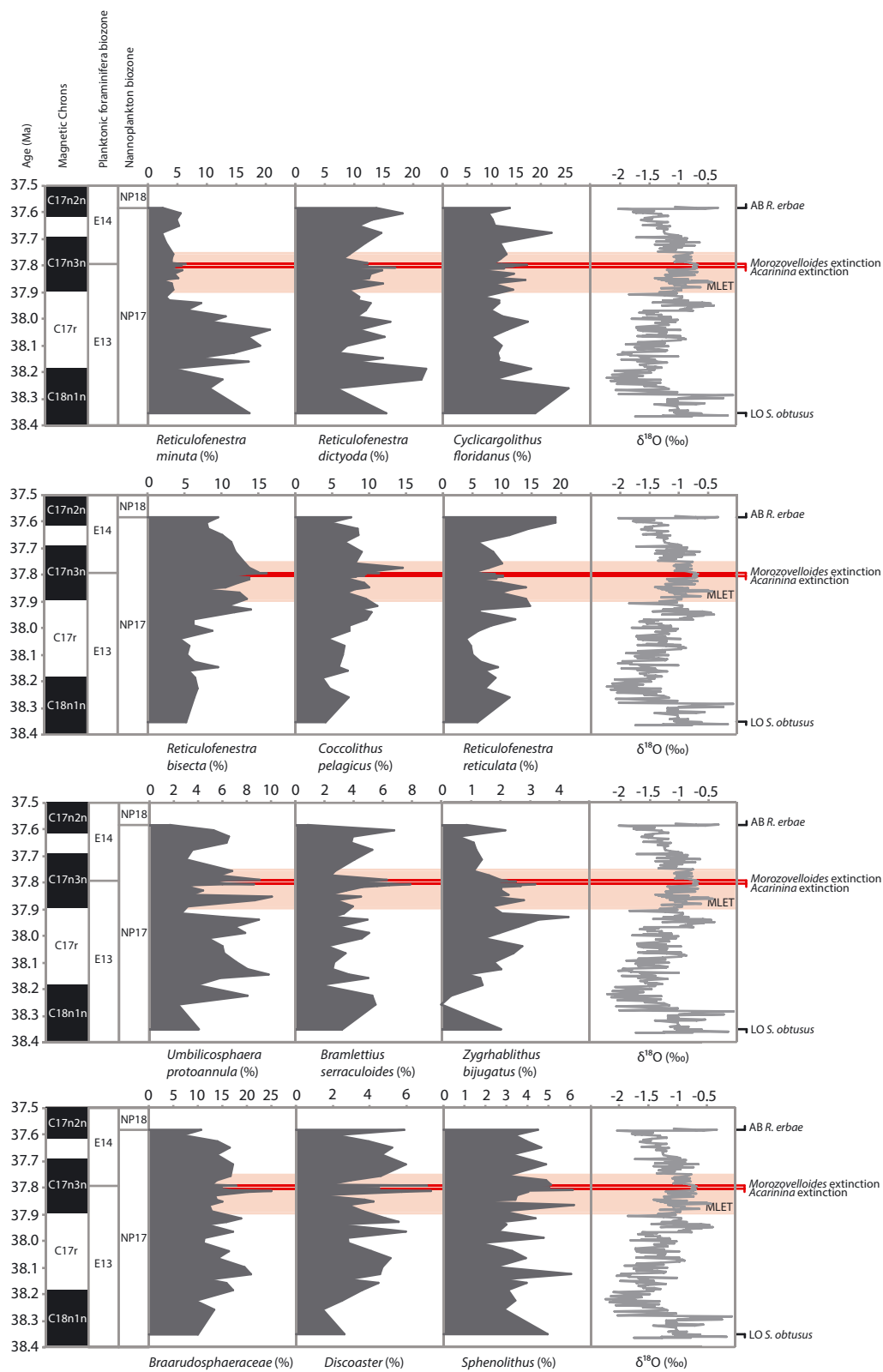
Fig. 2. Calcareous nannoplankton main species relative abundances across the Middle/Late Eocene Turnover event plotted against planktonic foraminiferal oxygen isotope data from Wade and Kroon (2002; species data has been merged to form a time series). Nannofossil biostratigraphy from this study; Planktonic foraminifera biostratigraphy from Wade (2004); Magnetostratigraphy and age control from Pälike et al. (2001); MLET (shaded area) from Kamikuri and Wade (2012).

~38 Ma (from ~20 to 4%). The larger reticulofene-strids of the *R. dictyoda* group and *C. floridanus* are consistently abundant through the interval (~12 and ~13% respectively) but show no clear trends. The *Reticulofenestra reticulata* group (*Reticulofenestra erbae*, *Reticulofenestra reticulata* and *Reticulofenestra westerholdii*) demonstrate a gradual increase through the interval (~8 to 19%).

The *Coccolithus pelagicus* group (mostly *C. pelagicus* but including *Coccolithus eopelagicus* > 14 µm) and the *Reticulofenestra bisecta* group (including *Reticulofenestra stavensis* > 10 µm), both show similar, distinctive abundance trends (Fig. 2), with an increase to a peak during the MLET interval, at ~37.79 Ma (4 to 14.5% and 6 to 16%), followed by a gradual decrease to the top of the section (5 and 8%). Similarly, *Zygrhablithus bijugatus* increases (0 to 4.3%) to 37.93 Ma and then decreases through the upper part of the interval (to 0.6%). However, this holococcolith species is consistently rare (< 5%) and the trend is therefore less significant than groups that account for a greater proportion of the assemblage.

The Braarudosphaeraceae (*Braarudosphaera*, *Pemma*, *Micrantholithus*), comprise ~15% of the assemblages and while fluctuations can be up to 6%, there is no clear stratigraphic trend in the variability (Fig. 2).

Discoaster and *Sphenolithus* are consistently rare (1 to 7% in *Discoaster* and 1 to 6% in *Sphenolithus*), and though there are fluctuations there is no clear stratigraphic trend in the variability. Other taxa, such as, *Umbilicosphaera protoannula* and *Bramletteius serraculoides* have moderate abundances (6% and 4%, respectively) and large fluctuations (2 to 10% and 1 to 8%) but display no clear stratigraphic trends (Fig. 2).

The cold eutrophs group increase through the section, but contribute only 1 to 5% and show large fluctuations. The warm oligotrophs group show no clear trends through the section, averaging ~15% with a range from 19 to 7% (Fig. 3).

3.3 Statistical analysis

The first two DCA axes (DCA 1 and DCA 2) represent the majority of variation within the dataset: 44 and 22% respectively. The DCA plot (Fig. 4) highlights a distinct difference along the DCA 1 axis between pre-MLET assemblages and MLET and post-MLET assemblages. The overlain age, oxygen and carbon isotope vectors in the environmental fit also highlight that age is the main factor controlling variation along DCA 1 ($r^2 = 0.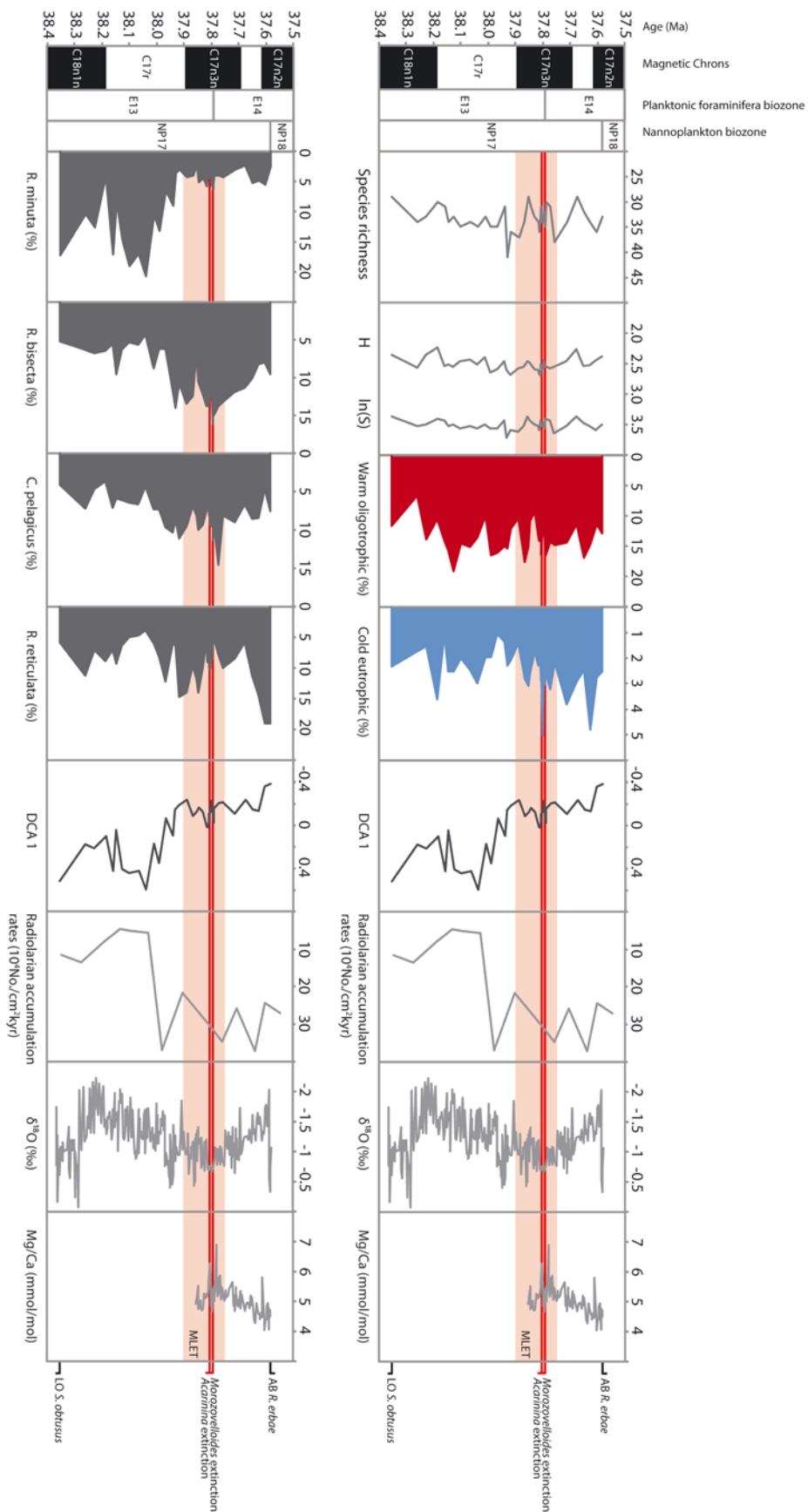54$, $p < 0.001$), with carbon isotopes control-ling some additional variation along this axis ($r^2 = 0.24$, $p < 0.008$). Oxygen isotopes correspond weakly to both DCA 1 and DCA 2 ($r^2 = 0.21$, $p < 0.012$). Plotting the DCA 1 values against age (Fig. 3) to assess the variation through time shows a clear shift between 38.04 and 37.93 Ma leading into the MLET event.

4. Discussion

The calcareous nannofossil populations at Blake Nose across the MLET and adjacent intervals are dominated by neritic (braarudosphaerids) and warm to temperate eurytopic and mesotrophic favouring taxa (e. g., reticulofenestrids and *Coccolithus*). Oligotrophs (discoasterales) and cooler-water-favouring eutrophs (*Chiasmolithus*, *Clausicoccus*) are subordinate. These assemblages indicate that varying but relatively meso-eutrophic, warm-water conditions prevailed throughout the interval. Although there are minor shifts in species abundance, the MLET interval itself does not stand out as exceptional, yet a distinct shift in DCA 1 implies a degree of assemblage change leading into the MLET event. No extinctions or originations are associated with the MLET interval, although the extinction of *Sphenolithus obtusus* occurs ~550 kyr before the event and the base of the *Reticulofenestra erbae* acme occurs ~200 kyr after.

The high abundances of braarudosphaerids indicate the strong influence of the neritic environment, to which these taxa are almost exclusively restricted. The precise features of the neritic environment which control the distribution of braarudosphaerids are not well understood but may include high nutrient load and life cycle stages that require shallower water (Bown 2005). No strong trends are seen in the braarudosphaerids abundance indicating that neritic water influence dominated throughout the interval. The short term variability in the abundance data most likely reflects natural instability in the neritic environment together with variability related to the location of this site close to the shelf/open-ocean interface. This may have included influence of the proto-Gulf Stream, whose strength and position, as well as associated eddies and related upwelling, may have increased environmental variability on a range of timescales (Wade and Kroon 2002, Huber et al. 2003, Okafor et al. 2009).

Previous oxygen isotope studies of this Blake Nose succession have documented a high variability record but with an overall cooling trend from approximately 38.2 Ma to 37.8 Ma (Wade and Kroon 2002), corres-

ponding to a cooling of ~6°C (Wade 2004). A trend to more negative $\delta^{18}O$ values above the MLET suggests a return to warmer conditions, but this is not supported by Mg/Ca records from this upper interval (Okafor et al. 2009). This discrepancy was attributed to variable $\delta^{18}O$ seawater values caused by weakening of the hydrological cycle (Okafor et al. 2009).

In addition, the highly variable geochemical records from Blake Nose have been attributed to variations in the Gulf Stream and its interaction with the Blake Plateau over time, for example, due to deflections and varying strengths of the current or associated eddies (Pinet et al. 1981, Wade and Kroon 2002). Reduced Gulf Stream influence at the site would have caused lower temperatures and salinities (Okafor et al. 2009), with only slight changes in the Gulf Stream position causing variability in the oxygen isotope record of 1‰ (Huber et al. 2003).

In general, the nannofossil assemblages show no strong evidence for a significant temperature shift at this time. The warm water, open-ocean favouring taxa, such as discoasters and sphenoliths, are rare throughout ($<5\%$) and show no significant abundance trends or covariance with the oxygen isotope records (Fig. 3). These taxa were likely at the limits of their optimum conditions and the high nutrient conditions and environmental instability of this neritic site dominated over the influence of temperature at this subtropical location.

Of the dominant reticulofenestrid groups, it is those taxa that favour warmer latitudes that show some of the highest abundances, e.g. *R. bisecta*, *R. reticulata* and *Cyclicargolithus*. *Reticulofenestra reticulata* increases in abundance at the base of the MLET and in the uppermost part of the section, and *R. bisecta* shows an increase across the MLET, similar to the trend in
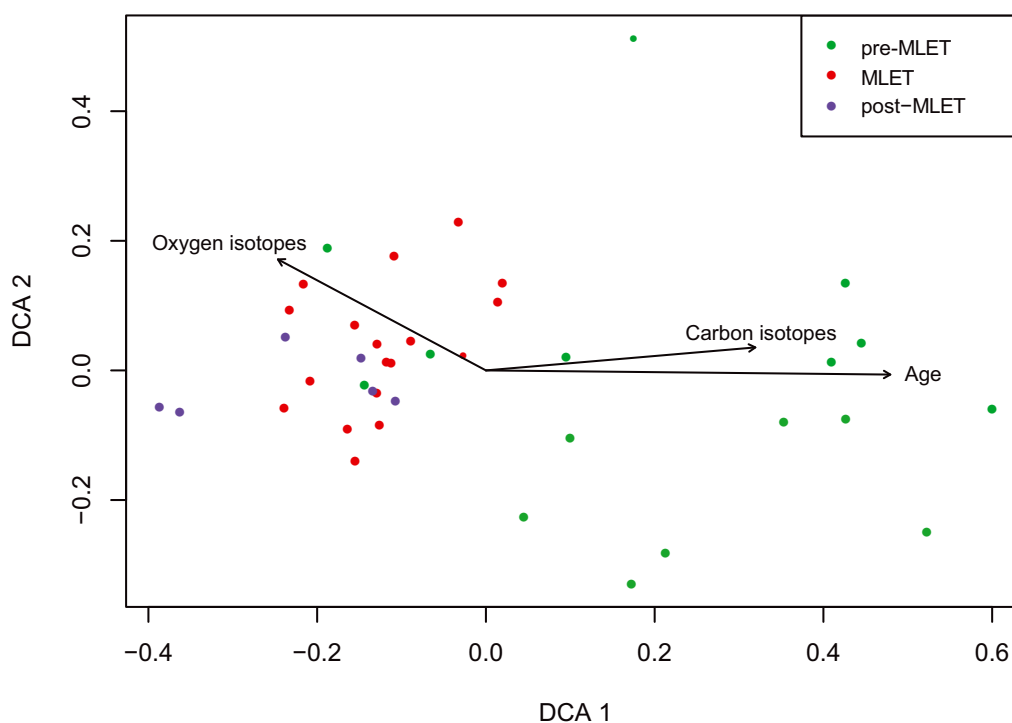
Fig. 4. DCA plot (axes 1 and 2) showing pre-MLET, MLET and post-MLET samples with overlain age, carbon and oxygen vectors.

Fig. 3. Calcareous nannoplankton species richness, SHE diversity plots, palaeoecology groups, DCA 1 sample scores and key nannofossil taxa plotted against radiolarian accumulation rates (Kamikuri and Wade 2012), the planktonic foraminiferal oxygen isotope data from Wade and Kroon (2002) and planktonic foraminiferal Mg/Ca data from Okafor et al. (2009). Nannofossil biostratigraphy from this study; Planktonic foraminifera biostratigraphy from Wade (2004); Magnetostratigraphy and age control from Pälike et al. (2001); MLET (shaded area) from Kamikuri and Wade (2012).

C. pelagicus (Fig. 3). Given the stable isotopes indicate cooling through this interval, this suggests a primary response to increasing nutrients and surface water productivity. The trophic preference of *R. reticulata* has been the subject of some discussion but has included interpretations of mesotrophy (Villa et al. 2008, Schneider et al. 2011, Shamrock and Watkins 2012). At the same time as these taxa were increasing, the small reticulofenestrid species, *R. minuta*, declines, which is intriguing, given this taxon is often considered an opportunistic cool-water favouring eutroph (Wade and Bown 2006). It is possible that due to this site's low latitude location, *R. minuta* was disadvantaged and less able to take advantage of the increased nutrients. A similar record of decline in *R. minuta* during an interval of increasing productivity was noted at a tropical site at the Eocene-Oligocene boundary (Dunkley Jones et al. 2008).

The DCA results highlight the assemblage change through the MLET. However, because both oxygen and carbon isotopes are only weakly correlated to DCA 1, the main environmental factor which controls variation through time (i.e. along DCA 1) is undetermined. The MLET is a minor cooling event so a weak correlation between the oxygen isotopes and the DCA axes is not unexpected. Furthermore, the DCA results support the species abundance plots which also show little correlation to the oxygen isotope data, thus implying that temperature was not an important driver of assemblage change across the interval. The stronger correlation of the carbon isotopes to DCA 1 may relate to the proposed nannoplankton response to changing nutrient conditions shown by increasing abundances of *R. bisecta, R. reticulata* and *C. pelagicus*. However, there is no significant change in the carbon isotopes through the MLET (Wade 2004), although there are only limited data available.

This interval of moderate nannofossil population shifts is coincident with a significant increase in radiolarian accumulation rate (Kamikuri and Wade 2012), providing further evidence of increased productivity at the base of the MLET. This may have been an important factor in the high turnover in radiolarians and extinction of planktonic foraminifera species. The radiolarians also show a minor decline in low and mid latitude taxa during the MLET interval and an increase in cosmopolitan forms. There is no clear comparative trend seen in the warm oligotrophic nannofossils though there is a minor, longer-term increase in cooler-water taxa through the study interval, with increasing values post-MLET corresponding to the cooling

shown by Mg/Ca values (Fig. 3). If anything, it is the warm-temperate favouring nannofossil taxa that increase at the MLET onset (*R. bisecta* and *C. pelagicus*) but again, this may be predominantly a response to increasing nutrients.

Subtle changes in preservation may also have affected the nannofossil assemblage although this was not evident in our LM observations. A large proportion of siliceous material was present throughout and the influx of radiolarians at the base of the MLET may have led to preservational differences and could explain the loss of the smaller, more fragile reticulofenestrids. Given our documentation of relatively consistent nannofossil preservation throughout the study section we do not consider this a significant factor in our abundance data.

4.1   Decoupling of plankton sensitivity across the MLET and other events

The lack of nannofossil origination or extinction events at the MLET contrasts with the high turnover of radiolarian taxa and extinction of two major planktonic foraminiferal groups. This clearly indicates that a higher level of environmental perturbation in the system is required to cause phytoplankton extinctions, relative to zooplankton. Heterogeneity of sensitivity in different plankton groups is a phenomenon that has been recently recognised in other Paleogene plankton data, with nannoplankton showing far less population variability than foraminifers and dinoflagellates through the environmental perturbations associated with the early Eocene hyperthermal events (Gibbs et al. 2012). Similarly, the Eocene-Oligocene transition is associated with a number of significant extinction events in planktonic foraminifera and a major taxonomic turnover in radiolaria (Wade and Pearson 2008, Kamikuri et al. 2012), and while there are associated assemblage shifts in the calcareous nannofossils (Dunkley Jones et al. 2008), there is not the same level of taxic turnover. This sensitivity contrast between plankton groups may relate to differing life strategies, with zooplankton residing at different depths in the water column (mixed layer to thermocline dwellers) or migrating through the water during different life cycle stages (Wade et al. 2008). Changes in water column structure, and in particular the breakdown of stratification and/or shallowing of the thermocline, as has been suggested for the MLET at Blake Nose, may lead to reduced habitat space for zooplankton species and accompanying extinction pres-

sure. Calcareous nannoplankton species by contrast appear less sensitive to water column partitioning (in general, although not exclusively) and so may be more resilient to the same magnitude of environmental change of this kind.

5.   Conclusions

Calcareous nannoplankton records across the MLET at Blake Nose show short-term abundance variations and a minor long-term increase in cool taxa but no coincident origination or extinction events. The dominance of neritic and warm to temperate eurytopic and mesotrophic taxa throughout indicate relatively productive and unstable surface water conditions at this subtropical location. Increases in the warm to temperate reticulofenestrid groups, *R.bisecta* and *R.reticulata*, at the base of the MLET interval suggest an increase in nutrient input, and this is coincident with an increase in radiolarian accumulation rates and radiolarian turnover. The closely spaced planktonic foraminifera extinction levels are not marked by any exceptional nannofossil response. These records illustrate the contrasting sensitivities to environmental change in these different plankton groups, with radiolarians acutely affected but only a muted response seen in the calcareous nannoplankton. This spectrum of sensitivity is revealed herein at the MLET but is also relevant to other global change events, such as the Eocene hyperthermals and the Eocene-Oligocene boundary onset of glaciation.

References

Agnini, C., Fornaciari, E., Raffi, I., Catanzariti, R., Pälike, H., Backman, J., Rio, D., 2014. Biozonation and biochronology of Paleogene calcareous nannofossils from low and middle latitudes. Newsletters on Stratigraphy **47**, 2, 131–181.

Agnini, C., Fornaciari, E., Giusberti, L., Grandesso, P., Lanci, L., Luciani, V., Muttoni, G., Pälike, H., Domenico, R., Spofforth, D.J.A., Stefani, C., 2011. Integrated biomagnetostratigraphy of the Alano section (NE Italy): A proposal for defining the middle-late Eocene boundary. GSA Bulletin 123, 5/6, 841–872, doi: 10.1130/B30158.1.

Bice, K.L., Sloan, L.C., Barron, E.J., 2000. Comparison of early Eocene isotopic paleotemperatures and the three-dimensional OGCM temperature field: The potential for use of model-derived surface water $\delta^{18}O$. In: Huber, B.T., MacLeod, K.G. & Wing, S.L., (Eds.), Warm climates in Earth history. Cambridge University Press, p.79–131.

Bown, P., Pearson, P., 2009. Calcareous plankton evolution and the Paleocene/Eocene thermal maximum event: New evidence from Tanzania. Marine Micropaleontology **71**, 60–70, doi: 10.1016/j.marmicro.2009.01.005.

Bown, P.R., Dunkley Jones, T., Lees, J.A., Pearson, P.N., Randell, R., Coxall, H.K., Mizzi, J., Nicholas, C., Karega, A., Singano, J., Wade, B.S., 2008. A calcareous microfossil Konservat Lagerstätte from the Paleogene Kilwa Group of coastal Tanzania. GSA Bulletin **120**, 3–12.

Bown, P.R., 2005. Early to Mid-Cretaceous calcareous nannoplankton from the Northwest Pacific Ocean, Leg 198, Shatsky Rise. In: Bralower, T.J., Premoli Silva, I., Malone, M.J. (Eds.), Proceedings of the Ocean Drilling Program, Scientific Results, vol.198, p.1–82.

Bown, P.R., Lees, J.A., Young, J.R., 2004. Calcareous nannoplankton evolution and diversity. In: Thierstein, H., Young, J.R. (Eds) Coccolithophores: from molecular processes to global impact, Springer-Verlag, p.481–508.

Bown, P.R., Young, J.R., 1998. Techniques. In: Bown, P.R., (Ed.), Calcareous Nannofossil Biostratigraphy. Kluwer Academic Publishers, p.16–28

Bralower, T.J., 2002. Evidence of surface water oligotrophy during the Palaeocene-Eocene thermal maximum: Nannofossil assemblage data from Ocean Drilling Program Site 690, Maud Rise, Weddell Sea. Paleoceanography **17**, doi: 10.1029/2001PA000662.

Buzas, M.A., Hayek, L.C., 1998. SHE analysis for biofacies identification. Journal of Foraminiferal Research **28**, 233–239.

Dunkley Jones, T., Bown, P.R., Pearson, P.N., Wade, B.S., Coxall, H.K., Lear, C.H., 2008. Major shifts in calcareous phytoplankton assemblages through the Eocene Oligocene transition of Tanzania and their implications for low-latitude primary production. Paleoceanography **23**, 4, doi: 10.1029/2008PA001640.

Fornaciari, E., Agnini, C., Catanzariti, R., Rio, D., Bolla, E.M., Valvasoni, E., 2010. Mid-Latitude calcareous nannofossil biostratigraphy and biochronology across the middle to late Eocene transition. Stratigraphy **7**, 4, 229–264.

Gibbs, S.J., Bown, P.R., Murphy, B.H., Sluijs, A., Edgar, K.M., Pälike, H., Bolton, C.T., Zachos, J.C., 2012. Scaled biotic disruption during early Eocene global warming events. Biogeosciences **9**, 4679–4688, doi: 10.5194/bg-9-4679-2012.

Gibbs, S.J., Bown, P.R., Sessa, J.A., Bralower, T.J., Wilson, P.A., 2006. Nannoplankton extinction and origination across the Paleocene-Eocene Thermal Maximum. Science **314**, 1770–1773, doi: 10.1126/science.1133902.

Haq, B. U., 1980. Biogeographic history of Miocene calcareous nannoplankton and paleoceanography of the Atlantic Ocean. Micropaleontology **26**, 414–443.

Haq, B. U., Lohmann, G. P., 1976. Early Cenozoic calcareous nannoplankton biogeography of the Atlantic Ocean. Marine Micropaleontology **1**, 119–194.

Herrle, J. O., 2002. Paleoceanographic and Paleoclimatic Implications on Mid-Cretaceous Black Shale Formation in the Vocontian Basin and the Atlantic: Evidence from Calcareous Nannofossils and Stable Isotopes. Ph. D. Thesis, University of Tübingen, Germany, 114 p.

Huber, M., Sloan, L. C., Shellito, C., 2003. Early Palaeogene ocean and climate: A fully coupled modelling approach using the NCAR CCSM. In: Wing, S. L., Gingerich, P. D., Schmitz, B., Thomas, E., (Eds.), Causes and Consequences of Globally Warm Climates in the Early Paleogene. Geological Society of America Special Paper 369, 25–47.

Kamikuri, S., Moore, T. C., Ogane, K., Suzuki, N., Pälike, H., Nishi, H. 2012. Early Eocene to early Miocene radiolarian biostratigraphy for the low-latitude Pacific Ocean. Stratigraphy **9**, 1, 77–108.

Kamikuri, S., Wade, B. S., 2012. Radiolarian magnetobiochronology and faunal turnover across the middle/late Eocene boundary at Ocean Drilling Program Site 1052 in the western North Atlantic Ocean. Marine Micropaleontology 88–89, 41–53.

Kroon, D., Norris, R. D., Klaus, A., 1998. Drilling Blake Nose: the search for evidence of extreme Palaeogene – Cretaceous climates and extraterrestrial events. Geology Today, **14**, 22–226.

Lees, J. A., Bown, P. R., Young, J. R., Riding, J. B., 2004. Evidence for annual records of phytoplankton productivity in the Kimmeridge Clay Formation coccolith stone bands (Upper Jurassic, Dorset, UK). Marine Micropaleontology **52**, 29–49.

Martini, E., 1971. Standard Tertiary and Quaternary calcareous nannoplankton zonation. In: Farinacci, A. (Ed.), Proceedings 2nd International Conference Planktonic Microfossils Roma, Rome **2**, p. 739–785.

Norris, R. D., Kroon, D., Klaus, A., 1998. Chapter 1: Site 1052. In: Proceedings of the Ocean Drilling Program, Initial Reports, 171B, p. 5–10.

Ogg, J. G. & Bardott, L. 2001. Aptian through Eocene magnetostratigraphic correlation of the Blake Nose transect (Leg 171B), Florida Continental Margin. In: Norris, R. D., Kroon, D., Klaus, A., (Eds.), Proceedings of the Ocean Drilling Program, Scientific Results, vol. **171B**. Ocean Drilling Program, College Station, TX, p. 1–58.

Okafor, C. U., Thomas, D. J., Wade, B. S., Firth, J., 2009. Environmental change in the subtropics during the late middle Eocene greenhouse and global implications. Geochemistry, Geophysics, Geosystems 10, 7, 1–13.

Pälike, H., Shackleton, N. J., Röhl, U., 2001. Astronomical forcing in late Eocene marine sediments. Earth and Planetary Science Letters, **193**, 3–4, 589–602.

Pinet, P. R., Popenoe, P., Nelligan, D. F., 1981. Gulf Stream: Reconstruction of Cenozoic flow patterns over the Blake Plateau. Geology 9, 266–270.

Roth, P. H., Krumbach, K. R., 1986. Middle Cretaceous calcareous nannofossil biogeography and preservation in the Atlantic and Indian oceans: Implications for paleoceanography. Marine Micropaleontology **10**, 1–3, 235–266, doi: 10.1016/0377-8398(86)90031-9.

Schneider, L. J., Bralower, T. J., Kump, L. R., Patzkowsky, M. E., 2013. Calcareous nannoplankton ecology and community change across the Paleocene-Eocene Thermal Maximum. Paleobiology **39**, 4, 628–647, doi: 10.1666/12050.

Schneider, L. J., Bralower, T. J., Kump, L. R., 2011. Response of nannoplankton to early Eocene ocean destratification. Palaeogeography, Palaeoclimatology, Palaeoecology **310**, 152–162, doi: 10.1016/j.palaeo.2011.06.018.

Shamrock, J. L., Watkins, D. K., 2012. Eocene calcareous nannofossil biostratigraphy and community structure from Exmouth Plateau, Eastern Indian Ocean (ODP Site 762). Stratigraphy **9**, 1, 1–54.

Villa, G., Fioroni, C., Pea, L., Bohaty, S., Perisco, D., 2008. Middle Eocene-late Oligocene climate variability: Calcareous nannofossil response at Kerguelen Plateau, Site 748. Marine Micropaleontology **69**, 173–192.

Wade, B. S., Premec Fucek, V., Kamikuri, S., Bartol, M., Luciani, V., Pearson, P. N., 2012. Successive extinctions of muricate planktonic foraminifera (*Morozovelloides* and *Acarinina*) mark the base Priabonian. Newsletters on Stratigraphy **45**, 245–262, doi: 10.1127/0078-0421/2012/0023.

Wade, B. S., Olsson, R. K., 2009. Investigation of pre-extinction dwarfing in Cenozoic planktonic foraminifera. Palaeogeography, Palaeoclimatology, Palaeoecology, 284, 39–46.

Wade, B. S., Al-Sabouni, N., Hemleben, C., Kroon, D., 2008. Symbiont bleaching in fossil planktonic foraminifera. Evolutionary Ecology **22**, 253–265, doi: 10.1007/s10682-007-9176-6.

Wade, B. S., Pearson, P. N., 2008. Planktonic foraminiferal turnover, diversity fluctuations and geochemistry across the Eocene/Oligocene boundary in Tanzania. Marine Micropaleontology **68**, 244–255, doi: 10.1016/j.marmicro.2008.04.002.

Wade, B. S., Bown, P. R., 2006. Calcareous nannofossils in extreme environments: The Messinian Salinity Crisis, Polemi Basin, Cyprus. Palaeogeography, Palaeoclimatology, Palaeoecology 233, 271–286.

Wade, B. S., 2004. Planktonic foraminiferal biostratigraphy and mechanisms in the extinction of Morozovella in the late middle Eocene. Marine Micropaleontology 51, 23–38.

Wade, B. S., Kroon, D., 2002. Middle Eocene regional climate instability: Evidence from the western North Atlantic. Geology 30, 11, 1011–1014.

Wei, W., Villa, G., Wise, S. W., 1992. Paleoceanographic implications of Eocene-Oligocene calcareous nannofossils from Sites 711 and 748 in the Indian Ocean. In: Wise, S. W., Schlich, R., (Eds.), Proceedings of the Ocean Drilling Program, Scientific Results, vol. **120**, p. 979–999.

Wei, W., Wise, S. W., 1990. Biogeographic gradients of middle Eocene-Oligocene calcareous nannoplankton in the South Atlantic Ocean. Palaeogeography, Palaeoclimatology, Palaeoecology **79**, 29–61.

Winter, A., Jordan, R. W., Roth, P. H., 1994. Biogeography of living coccolithophores in ocean waters. In: Winter, A. & Siesser, W. G. (Eds.), Coccolithophores, Cambridge University Press, p. 161–178.

Zachos, J., Pagani, M., Sloan, L., Thomas, E., Billups, K., 2001. Trend, Rhythms, and Aberrations in Global Climate 65 Ma to Present. Science **292**, 686–693.